Drag force approach to the transport of colloids in unsaturated soils

Peter F. Germann and Abdallah Alaoui
Soil Science Section, Department of Geography, University of Bern, Bern, Switzerland

Dagmar Riesen
BCD GmbH, Bern, Switzerland

Received 29 June 2001; revised 19 June 2002; accepted 19 June 2002; published 18 October 2002.

[1] A drag force approach to the transport of colloids in unsaturated soils is introduced. It is based on film flow which is due to momentum dissipation during porous media flow. Supporting results are from three types of colloid transport experiments: (1) sprinkling of a latex bead and methylene blue suspension in situ on the surface of a forest soil with subsequent bead collection underneath, (2) application of bead suspension to a column of undisturbed soil and purging of retained beads, and (3) application of a suspension with 5 bacteriophages to a different soil column. Relative colloid breakthrough concentrations in relation to the drag forces, P/P_0, versus $F_d(t)/A$, were well pronounced during bead breakthrough, and bead diameters had no significant impact. In contrast, phage breakthrough showed a wide range of behavior. Previous bacteria breakthrough experiments support the approach; however, site-specific soil properties should also be considered. *INDEX TERMS:* 1832 Hydrology: Groundwater transport; 1836 Hydrology: Hydrologic budget (1655); 1875 Hydrology: Unsaturated zone; *KEYWORDS:* colloid transport, film flow, macropore flow, momentum dissipation, preferential flow, unsaturated soils

Citation: Germann, P. F., A. Alaoui, and D. Riesen, Drag force approach to the transport of colloids in unsaturated soils, *Water Resour. Res.*, *38*(10), 1200, doi:10.1029/2001WR000744, 2002.

1. Introduction

[2] Retention and translocation of colloids are the two principle aspects of the water-borne colloid transport in soils and similar porous media. Straining, bridging, sorption, and sieving are among the retention processes. Matrix geometry, the physical and chemical properties of the colloid and matrix surfaces, and the chemical composition of the liquid govern retention. Translocation is due to the forces exerted from the moving water on the colloids.

[3] *Rahe et al.* [1978] found *Escherichia coli* bacteria to have moved in a sloping forest soil over a distance of at least 15 m within one hour of suspension application. *Gerba and Bitton* [1984], for instance, reported from groundwater flow studies that the bulk of larger *Escherichia coli* bacteria appeared about one hour earlier in an observation well 160 m downstream from an injection well than the bulk of the much smaller virus coliphage f2. Moreover, laboratory breakthrough experiments have demonstrated that microbial retention is much less effective in soils with undisturbed structures, and that some pores act as rapid flow conduits for colloid transport [e.g., *Smith et al.*, 1985; *Germann et al.*, 1987; *White*, 1985; *Jacobson et al.*, 1997; *Seta and Karathanasis*, 1997].

[4] In their extended review on particle transport through porous media *McDowell-Boyer et al.* [1986] focused on filtration theory, that is, mainly on the particles which are retained. However, they concluded that macropores may constitute the only functioning pathways for particle transport through fine-textured clay soils. Commenting on their review, *Germann and Douglas* [1987] regretted that *McDowell-Boyer et al.* [1986] did not more strongly asked for adequate hydrodynamic approaches to water flow in porous media which should include momentum of flow.

[5] Convection-dispersion, CD, is considered a major process for transporting colloids in reconstituted water-saturated sand columns, and in columns of undisturbed saturated and nonsaturated soils as put forward, for instance, by *Hornberger et al.* [1992], *Corapcioglu and Choi* [1996], and *Grolimund et al.* [2001]. These studies assumed the participation of entire soil moisture in the flow and transport of colloids. As a consequence total pore volume, PV, becomes an important parameter in estimating average flow and transport velocities. *Toran and Palumbo* [1992] found retardation factors less than unity in their CD-approach to the transport of bacteria which indicates preferred translocation. However, neither filtration nor CD can explain the fast microbial transport as reported by *Rahe et al.* [1978] and *Gerba and Bitton* [1984].

[6] Various studies proposed the separation of the pore space into the three regions gas-phase, and mobile and immobile water contents to better explain rapid transport phenomena in porous media. In most cases the two liquid phases are separated according to model calibration versus observed transport phenomena. *Gvirtzman and Gorelick* [1991], for instance, studied the transport of tritium, chloride and sulphate through the vadose zone to the unconfined

0043-1397/02/2001WR000744$09.00

groundwater table at about 28 m below the surface. They inferred the volumetric separation between mobile and immobile water from the advanced propagation of the two anions when compared with the transport of tritium which is considered to trace the flow of water. Advanced propagation of the anions was due to their exclusion from negatively charged clay minerals. The authors assumed steady flow from 2 m below the surface to the groundwater table over a period of 27 years. They tested a hydrodynamic CD-model in which water exchange was with the entire soil moisture θ of 0.19 m^3 m^{-3}, but anion exchange occurred only in its mobile phase, θ_m, of 0.11 and 0.09 m^3 m^{-3} for chloride and sulphate, respectively. To a second model they added a term which accounted for anion exchange with the immobile portion of soil moisture. They found the immobile portion, θ_{im}, to be 0.023 and 0.019 m^3 m^{-3} for the two anions studied, and the corresponding exchange volumes, θ_{ex}, amounted to 0.061 and 0.084 m^3 m^{-3}, respectively. Total soil moisture θ_m was measured whereas θ_m, θ_{im}, and θ_{ex} followed from the calibration of the model against the depth distributions of the anions. Model constrictions always confine the separated moisture volume fractions to "reasonable" ranges which degrade this and similar concepts to a mere calibration procedure. It is conceivable that the application of different numerical techniques to solve the CD-equations may lead to different fractions of θ_m, θ_{im}, and θ_{ex}. The discussion indicates the need for an independent assessment of the effects of mobile soil moisture on colloid transport. Moreover, transient processes need to be considered when studying particle transport between the soil surface and the 2-m depth.

[7] *Rehman et al.* [1999] approached virus transport over long distances in aquifers with a first-order spectral perturbation analysis. Their stochastic variations of the flow parameters in some model calculations resulted in faster virus propagation in comparison with the average velocity of the water flow. *Ginn* [2000] admitted to the faster propagation of the virus, however, the formulation of the mathematical model did a priori not allow for faster virus advancement and he thus qualified the modeling results as artifacts.

[8] *Wan and Tokunaga* [1997] developed a theory on film straining during the transport of colloids in unsaturated porous media which they tested against break through experiments in columns of uniform quartz beads. They successfully applied the *Richards* [1931] equation to water flow and related particle straining with it. In a follow-up study *Veerapaneni et al.* [2000] demonstrated the impact of film flow on the transport of particles. They stressed the forces acting on single particles during film flow in porous media by distinguishing three cases of particle motion: (1) completely submerged sphere with a diameter smaller than film thickness; (2) sphere with a diameter comparable to but smaller than film thickness; (3) partially submerged sphere. They calibrated the approach against experimental results obtained from film flow and related transport of particles along an inclined plate of smooth glass. The thickness of the liquid films varied between 122 and 672 μm and the particle diameters were in the range of 20 to 1000 μm. They considered forces of shear, translation, rotation, gravity, and friction in cases 1 and 2, and included capillarity between the particle, liquid, and air in case 3. The intricate model was successfully applied to cases 1 and 2. The application established a strong relation between the ratio of particle velocity to maximum fluid velocity on one side and the ratio of particle diameter to film thickness on the other side as long as the latter ratio did not exceed 0.8.

[9] *Grolimund and Berkovec* [2001] stressed the importance of traveling chromatographic fronts on colloid transport in soils. *Wan and Wilson* [1992] demonstrated in artificial and unsaturated porous media that the moving water-air interfaces scooped and shoved particles along with the wetting front, thus supporting Grolimund and Berkovec's statement who also considered the fronts to elongate the tails of the colloid breakthrough curves. In addition, *Grolimund and Berkovec* [2001] suggested first-order kinetics of colloid mobilization inappropriate as they were explored, for instance, by *Saiers et al.* [1994]. Although *Grolimund and Berkovec* [2001] recognized the traveling fronts being important for pushing colloids through soils, they did not independently explore the fluid mechanical significance of front movement. *Schäfer et al.* [1998] concluded that "...the bacterial affinity to air-water interfaces is larger than their affinity to solid surfaces..." and thus they postulated that "...an exact description of the hydraulic properties helps to characterize the flow properties of the system." In accord with their conclusion we propose to analyze the dynamics of transient flow independently from the observed transport of colloids in undisturbed soils and to synthesize the two aspects later on rather to calibrate the former process to simply match the latter.

[10] *Germann and Di Pietro* [1999] presented the concept of momentum dissipation during transient flow in undisturbed soils. *Germann et al.* [2002] demonstrated that mobile soil moisture corresponds with the amplitude of temporal soil moisture variations during transient infiltration as measured, for instance, with TDR equipment. The traveling fronts are related with water films flowing along preferred flow paths, and the films are thought to exert drag forces onto the colloids, thus moving them through soils.

[11] Here, we are introducing a drag force approach to the transient transport of colloids through unsaturated and undisturbed soils. Further, we are elucidating its applicability to the transport of latex beads and bacteriophages.

2. Theory

[12] There are two kinds of approaches to water flow in unsaturated soils. The first kind is related to the potential gradients, mainly to those of capillarity and gravity. It involves total soil moisture and leads to the diffusion of capillary potential as it is expressed, for instance, in the *Richards* [1931] equation. There is a reversible relation between soil moisture and its capillary potential under consideration of hysteresis effects. A mandatory prerequisite are pores in which viscosity completely disperses momentum within a representative elementary volume, REV, as *Germann and Di Pietro* [1999] presented.

[13] The second kind of water flow in unsaturated soils involves only a small fraction of soil moisture which quickly reacts on sudden impacts. The generated kinetic energy must be strong enough to carry flow along a significant distance and with a significant rate. A mandatory prerequisite are continuous pores extending over depth ranges many times longer than the REV for diffusive flow.

These pores will be referred to as preferred flow paths and the process as preferential flow. Some of the momentum dissipates along the flow paths whereas the remainder results in a net drag force pushing colloids through unsaturated soils. Some of the colloids are moved due to sufficient impact while others get stuck in regions that are not exposed to dragging. Sieving and sorption to solid surfaces are additional processes of retaining particles in soils.

[14] The drag forces follow from a momentum dissipation approach to flow in structured field soils as proposed by *Germann and Di Pietro* [1999]. The basic theory led them to a kinematic wave approach to flow in structured soils, and the method of characteristics is applied to solve the associated differential transport equation. The approach was validated in situ and in columns of undisturbed soils against soil moisture variations obtained from rapid TDR-measurements and drainage flow, respectively, during and shortly after sprinkling at soil surfaces. Typically, less than 0.1 $m^3\ m^{-3}$ of soil moisture participated in the flow process [*Germann*, 2001].

[15] From fundamentals of fluid mechanics follows the kinetic energy of the moving water, w, per unit cross sectional area of soil, A m^2, and per unit path length dz m, which produces a specific drag force

$$\frac{F_d(t)}{A} = \frac{1}{2} \cdot \rho \cdot w \cdot v(t)^2 \tag{1}$$

(N m^{-2}). We consider F_d/A the dominant force which drives particles through soils at the macroscopic scale of A. Further, ρ (kg m^{-3}) is the fluid density, $v(t) = q(t)/w(t)$ m s^{-1} is the average velocity of the volume flux density of preferential flow, $q(t)$ (m s^{-1}), and $w(t)$ ($m^3\ m^{-3}$) is mobile soil moisture related with $q(t)$. (Note: $w \ll \theta$ $m^3\ m^{-3}$, where the latter is total soil moisture.) Sorption, sedimentation and sieving of the particles are thought to act against F_d/A.

[16] Mobile soil moisture is considered to flow in films and rivulets along pores of approximate uniform shapes which extend in the general direction of flow over lengths of centimeters to meters. These pores are referred to as macropores or paths of preferential flow. Newton's law of shear describes the velocity profile within a film of water which flows in a laminar fashion, and *Germann and Di Pietro* [1999], among others, derived the following relation from it:

$$q = b \cdot w^a, \tag{2}$$

where b (m s^{-1}) is conductance and the dimensionless exponent is $a = 2$ for flow in a cylindrical tube which corresponds to Hagen Poiseuille's law. Laminar water flow along a plane or in a planar fissure results in $a = 3$ (i.e., the "cubic law" according to *Shrauf and Evans* [1986]). Equation (2) is the basic expression of a kinematic wave according to theory of *Lighthill and Whitham* [1955] who solved its various stages with the method of characteristics as demonstrated below. Further, from dimensional analysis follows for gravity driven, vertical, and laminar film flow that

$$b = \frac{g}{2 \cdot a \cdot \eta} \frac{A^2}{\ell^2}, \tag{3}$$

where g (m s^{-2}) is acceleration due to gravity, η ($m^2\ s^{-1}$) is kinematic viscosity, and ℓ m is the length of contact within A between w and the parts at rest which consist either of stagnant water or the solids of the soil matrix. In addition,

$$w = \frac{\ell \cdot W}{A}, \tag{4}$$

where W m is the average thickness of the moving water films. Average velocity of flow is

$$v(t) = \frac{q(t)}{w(t)} = b^{1/a} \cdot q(t)^{(a-1)/a} \tag{5}$$

(m s^{-1}). The combination of Equations (1) and (5) leads to

$$\frac{F_d(t)}{A} = \frac{1}{2}\rho \cdot b^{1/a} \cdot q(t)^{(2a-1)/a} = \frac{1}{2}\rho \cdot b^2 \cdot w^{2a-1} \tag{6}$$

Pa.

[17] The expressions for transient laminar flow in structured and nonsaturated soils are now presented. Water is assumed to infiltrate as a rectangular pulse with volume flux density q_S (m s^{-1}) and duration t_S (s), leading to the initial and boundary conditions of

$$t \le 0 \text{ and } t \ge t_S : q(0,t) = w(0,t) = 0 \tag{7a}$$

$$0 \le t \le t_S : \qquad q(0,t) = q_S; \qquad w(0,t) = w_S = \left[\frac{q_S}{b}\right]^{1/a} \tag{7b}$$

$$0 \le z \le \infty : \qquad q(z,0) = w(z,0) = 0. \tag{7c}$$

[18] Figure 1a illustrates temporal mobile soil moisture variations, $w(z, t)$, at various depths during the passing of a kinematic wave, and Figure 1b its depth variation at various times. In the following, we introduce the propagations of the wetting and draining fronts which are dealt with the method of characteristics. Three phases can be distinguished.

2.1. Phase 1: Steady Flow Between the Wetting Front and the Surface

[19] The average velocity equals the velocity of the wetting shock front, thus $v_w(t) = v(t)$. Under the assumption that the wetting-shock front does not disperse, its position follows from equation (5) as

$$z_W(t) = t \cdot b \cdot w^{(a-1)} = t \cdot b^{1/a} \cdot q^{(a-1)/a}. \tag{8}$$

The time lapsed for the wetting front to move to depth Z m is

$$t_W(Z) = \frac{Z}{b \cdot w_S^{(a-1)}} = \frac{Z}{b^{1/a} \cdot q_S^{(a-1)/a}}. \tag{9}$$

Equations (8) and (9) are the characteristic functions of the wetting front, as shown in Figure 1c.

2.2. Phase 2: Flow Between the Draining Front and the Surface

[20] At the moment of input cessation at $t = t_S$, a draining front moves with the velocity

$$v_D = \frac{dq}{dw} = a \cdot b \cdot w^{(a-1)} = a \cdot b^{1/a} \cdot q^{(a-1)/a}. \tag{10}$$

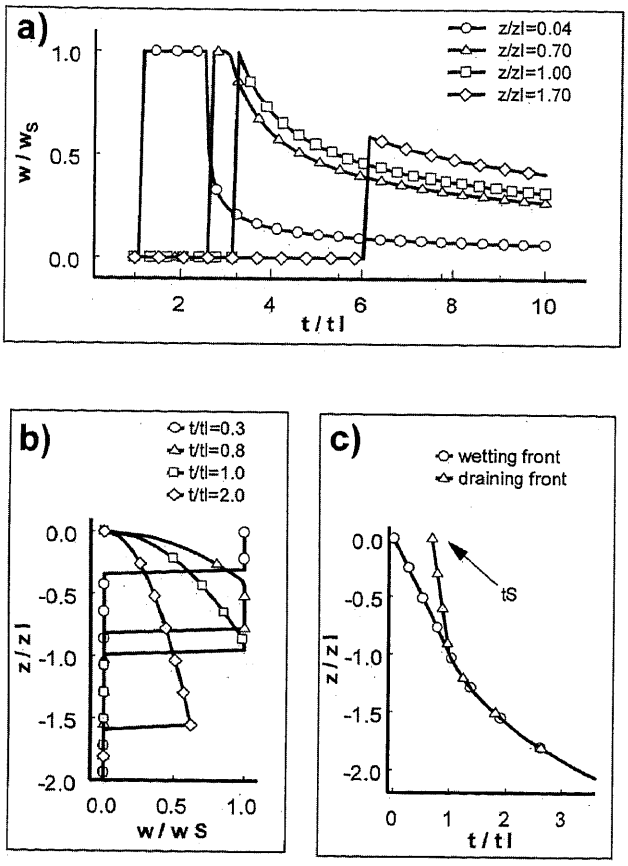

Figure 1. Schematic presentation of the kinematic wave model. (a) Temporal variation of mobile soil moisture at four depths. (b) depth variation of mobile soil moisture at four different times. (c) Characteristics of the wetting and draining fronts.

The position of the draining front is

$$z_D(t) = (t - t_S) \cdot a \cdot b \cdot w^{(a-1)} = (t - t_S) \cdot a \cdot b^{1/a} \cdot q^{(a-1)/a} \quad (11)$$

and the time lapsed for the draining front to move to Z is

$$t_D(Z) = t_S + \frac{Z}{a \cdot b \cdot w_S^{(a-1)}} = t_S + \frac{Z}{a \cdot b^{1/a} \cdot q_S^{(a-1)/a}}. \quad (12)$$

Equations (11) and (12) are the characteristic functions of the draining front, as illustrated in Figure 1c. A trailing wave evolves in the depth range of $0 \leq z \leq z_D(t)$, along which mobile moisture increases from $w(0) = 0$ to $w(z_D) = w_S$. The trailing wave is defined within the limits of $0 \leq z \leq z_D(t)$ and $t_S \leq t < \infty$ as

$$w(z,t) = \left[\frac{z}{a \cdot b \cdot (t - t_S)}\right]^{1/(a-1)} \quad (13)$$

After the passing of the draining front at Z and a time $t_D(Z)$, volume flux density and mobile soil moisture are

$$q(Z,t) = q_S \cdot \left(\frac{t_D(Z) - t_S}{t - t_S}\right)^{a/(a-1)} \quad (14)$$

and

$$w(Z,t) = w_S \cdot \left(\frac{t_D(Z) - t_S}{t - t_S}\right)^{1/(a-1)}, \quad (15)$$

respectively.

Table 1. Properties of Bantiger Soil (*Orthic Luvisol*)

Depth, m	Texture	Porosity E, $m^3\ m^{-3}$	Saturated Hydraulic Conductivity K_S, $m\ s^{-1}$
0.1–0.2	sandy loam	0.53	3.1×10^{-2}
0.2–0.25	sandy loam	0.41	1.1×10^{-2}
0.25–0.45	sandy loam	0.50	3.8×10^{-3}
0.45–0.55	sandy loam	0.42	2.3×10^{-2}

Table 2. Diameters and Total Numbers of Particles Infiltrated Into Bantiger Soil

Particle	Field Experiments Bantiger1		Soil Column Experiment Bantiger 2, Run1	
	Diameter, μm	Number of Particles	Diameter, μm	Number of Particles
YG	0.51	3.4×10^{11}	0.21	1.6×10^{11}
PC-Red	1.00	4.5×10^{10}	1.00	6.4×10^{10}
BB	1.75	8.5×10^{9}	1.67	6.0×10^{12}

2.3. Phase 3: Deceleration After Front Interception

[21] Because $v_D = a \cdot v_W$, equations (5) and (10), the draining front intercepts the wetting front at time

$$t_I = t_S \frac{a}{a-1} \quad (16)$$

s and at depth

$$z_I = \frac{a}{a-1} \cdot t_S \cdot b^{1/a} \cdot q^{(a-1)/a} = \frac{a}{a-1} \cdot t_S \cdot b \cdot w^{(a-1)} \quad (17)$$

m. Equations (16) and (17) indicate that time and depth of interception depend directly on the duration of water input to the soil surface, t_S. They are thus controlled by the experiment. For the sake of simplicity, we limited the analysis to the depth range of $0 \leq z < z_I$ because infiltration lasted always long enough to secure $Z_{max} < z_I$, where Z_{max} is the lowest depth of investigation. Figure 1c shows the front characteristic beyond the point (z_I, t_I) according, for instance, to *Germann* [1985].

[22] *Di Pietro and LaFolie* [1991] and *Mdaghri-Alaoui* [1998] derived the model parameters a and b from fitting the approach to experimental drainage flow and moisture variation data, respectively, by linearizing equations (14) and (15) to the form of

$$Y_i = V(q \text{ or } w) + U(q \text{ or } w)X_i, \quad (18)$$

where the index i indicates measurements and (q or w) indicates either the q- or the w-version of the slope and the

Table 3. Properties of Colombier Soil (*Calcaric Fluvisol*)

Depth, m	Texture	Porosity E, $m^3\ m^{-3}$	Saturated Hydraulic Conductivity K_S, $m\ s^{-1}$
0–0.08	clay loam	0.58	2.5×10^{-5}
0.08–0.28	clay loam	0.59	1.1×10^{-5}
0.28–0.36	clay loam	0.56	1.3×10^{-5}
0.36–0.44	sandy clay loam	0.50	8.3×10^{-6}
0.44–0.60	sandy loam	0.47	8.3×10^{-6}
0.60–0.70	sandy loam	0.49	2.5×10^{-5}

intercept, respectively. They are used to estimate the model parameters a and b, and the arrival time of the draining front at depth Z, $t_D(Z)$, according to the following procedure. From equations (14) and (15) follows

$$\ln[q(Z,t_i)/q_S] = \frac{a}{a-1}\ln[t_D(Z)-t_S] - \frac{a}{a-1}\ln[t_i - t_S] \quad (19)$$

and

$$\ln[w(Z,t_i)/w_S] = \frac{1}{a-1}\ln[t_D(Z)-t_S] - \frac{1}{a-1}\ln[t_i - t_S], \quad (20)$$

respectively. It follows that

$$a = \frac{U(q)}{U(q)+1} = \frac{U(w)-1}{U(w)}, \quad (21)$$

$$t_D(Z) = t_S + e^{-V/U}, \quad (22)$$

and

$$b = \frac{Z}{a \cdot q_S^{(a-1)/a} \cdot (t_D - t_S)} = \frac{Z}{a \cdot w_S^{(a-1)} \cdot (t_D - t_S)} \quad (23)$$

3. Experiments

3.1. General

[23] The results of three experiments are reported here: (1) Experiment Bantiger 1: In-situ infiltration of dye and latex bead suspension into a forest soil with subsequent selected soil sampling. (2) Experiment Bantiger 2: In the laboratory, a similar bead suspension was infiltrated into a column of undisturbed soil from the same forest location. The column was then purged with bead-free water. Effluents were collected in fractions. (See *Riesen* [1995] for details). (3) Experiment Colombier: Infiltration into and collection of a suspension with five different bacteriophages, which was once applied to a column of an undisturbed soil containing a filtering layer of a sandy clay loam. (See *Mdaghri-Alaoui* [1998] for details).

3.2. Methods

3.2.1. Preparation of a Soil Column

[24] A stainless steel cylinder (0.30 m inner diameter and 0.25 m high) was driven about 0.15 m into the soil at the location of column preparation. The cylinder acted as guide for digging and carving out the soil column beneath it to a depth of about 0.9 m. The exposed soil column was then coated with several layers of fiberglass and polyester resin. Its bottom was cut even, cleaned and a stainless steel disk with square holes 70 × 70 mm was mounted as support. The column was suspended with ropes on the ceiling of the laboratory, leaving free access to its top and bottom for instrumentation.

3.2.2. Sprinkling and Flow Collection

[25] Input of water and particle suspensions to the soil surface was through 72 nozzles mounted on a rotating disc with a diameter of 0.3 m. The nozzles were connected via small tubes with a manifold to which a precision pump controlled intensity and duration of flow.

[26] A funnel, mounted to the bottom of the column, was hydraulically connected to an outflow sampler collecting equal volumes of effluent and draining them subsequently into a fraction sampler. The time intervals to fill the 20 mL sampling tubes were automatically recorded.

[27] Volumetric soil moisture, θ $m^3\ m^{-3}$, was measured automatically with TDR-wave guides at various depths within the columns. A wave-guide consisted of a pair of rods of stainless steel, with diameters and lengths of 6 mm and 0.3 m, respectively. An RF-Pulse transformer was used to stabilize the signal on the Tektronix 1502B cable tester. The wave guides were multiplexed with a SDMX50 50W Coax Multiplexer, which was controlled by a 21X Campbell Micrologger. The TDR-System was calibrated according to *Roth et al.* [1990] who separated the impact of the wave-guide geometry from the soil properties, such as bulk density and the content of clay and organic matter, on the dielectric number. The limit of significant differences among individual measurements with the same wave-guide was assessed at utmost 0.002 $m^3\ m^{-3}$. The time interval of TDR-measurements, Δt, was 300 s.

3.3. Experiments Bantiger 1 and 2

[28] The soil is classified as *Orhtic Luvisol* with abundant earthworm channels and roots to the 0.80-m depth. Litter was mainly from beech leaves (*Fagus sylvatica*), the mineral Ah-horizon is located between 0.15 and 0.25 m. The diffuse boundary between the B- and C-horizon is between 1.15 and 1.25 m deep. The texture is a sandy loam (Table 1) throughout the profile.

Table 4. Characteristics of Bacteriophages Infiltrated Into Colombier Soil

Type	Genus	ξ-Potential, mV	Host Bacteria	Particle, $m\ L^{-1}$
H40/1	Siphoviridae (type B1)	−42.0	H40	3.7×10^{10}
H4/4	n.a.	n.a.	n.a.	7.8×10^{10}
T7	Podoviridae	−31.7 (pH 7.4)	*E. Coli* B (ATCC11303)	6.0×10^{9}
H6/1	Levividae (type E1)	−50.1	H6	2.6×10^{9}
f1	Inovirus (Inoviridae)	−42.3 (pH 7.4)	*E. Coli* K12 (ATCC15766)	4.4×10^{11}

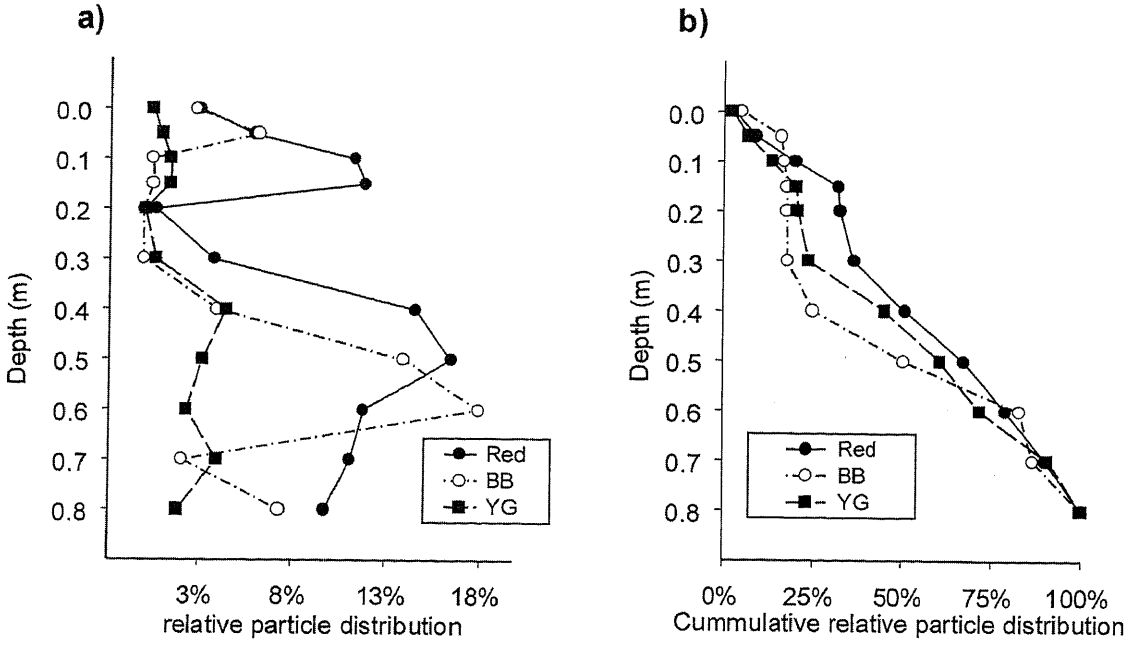

Figure 2. Experiment BANTIGER 1: In situ application of latex bead suspension. (a) Relative depth distribution of recovered particles (100% corresponds to the sum of particles recovered in the soil samples from the surface to the 0.8-m depth). (b) Cumulative relative depth distribution of recovered particles.

[29] For suspension and analysis of latex beads, a suspension containing the three different fluorescent latex beads YG, PC-Red, and BB (Table 2) was applied through the sprinkler. Each bead type was distinctly coated with a fluorescent dye, and the corresponding bead concentrations were analyzed with a fluorimeter, using calibration standards provided by the bead manufacturer. Accordingly, the three bead types had identical physicochemical properties. In particular, their surfaces were neutral of electrical charges and well buffered.

3.4. Experiment Bantiger 1: In Situ Experiment, Sampling of Latex Beads, and Sample Preparation

[30] Methylene Blue was added to the bead suspension according to Table 2. Rate and duration of suspension application were $q_S = 4.7 \times 10^{-5}$ m s^{-1} and $t_S = 1200$ s, respectively, amounting to a total volume of 4 L. The sprinkler was mounted in situ on the surface of the intact forest soil above the area of later sampling. Within less than an hour after suspension application, soil layers 50 mm thick were sequentially dug out underneath the sprinkled area. Soil samples were collected from the stained volumes and air-dried. In the laboratory, 10-g subsamples of each stained portion were dispersed in 50 mL solution of water and Alcopon (sodium hexa-meta-phosphate). After two days, the suspension was adjusted to pH 9, centrifuged at 5000 rpm and analyzed.

3.5. Experiment Bantiger 2: Laboratory Experiment With Latex Bead Suspension

[31] The composition of the applied particle suspension was according to Table 2. Infiltration run 1 included the particle suspension, and run 2 was with tap water without particles. Durations of infiltration were in both runs $t_S = 900$ s, and the rates of infiltration, q_S, were 3.9×10^{-5} and 4.4×10^{-5} m s^{-1}, respectively, in run 1 and run 2. The effluent was collected with the volume fraction sampler. Soil moisture was recorded with TDR-equipment, and the wave guides were inserted at depths of 0.08, 0.20, 0.45, and 0.70 m. The time interval of recording was set to $\Delta t = 300$ s.

3.6. Experiment Colombier: Laboratory Experiment With Bacteriophages Suspension

[32] The soil is classified as *Calcaric Fluvisol* from the Areuse delta near Neuchâtel (Switzerland). Porosity, soil organic matter, and pH vary between 0.47 to 0.59 m^3 m^{-3}, 2 and 5% by weight and 7 to 8, respectively. The texture between 0 and 0.36 m is a clay loam containing gravel and rock fragments; there is a sandy clay loam between the 0.36-m and the 0.44-m depth with somewhat reduced hydraulic conductivity, and a sandy loam between 0.44 and 0.70 m which is very low in coarse material. Mainly gravels were found below 0.7 m (Table 3).

3.6.1. Suspended Bacteriophages

[33] Five types of bacteriophages were simultaneously infiltrated into the soil column as listed in Table 4. The bacteriophages were counted with the double agar-layer technique. Isolation, counting, and purification of the phages were according to *Rossi* [1994].

[34] He also performed inactivation tests and adsorption experiments on them, using a standard buffered medium under constant agitation in the presence of montmorillonite. More than 90% of the phages were inactivated within 180 minutes obeying exponential decay. Phage H6/1 resisted the best, showed the lowest ξ potential and the highest hydrophobicity. Phages H40/1 and H6/1 did practically not react with the mineral colloids. In general, ξ potential, hydrophobicity, shape and size of phages were poorly correlated.

3.6.2. Instrumentation and Experiment

[35] Soil moisture was measured with the TDR-equipment. The wave guides were inserted at depths of 0.10, 0.30, 0.46 and 0.58 m. The time interval of recording was

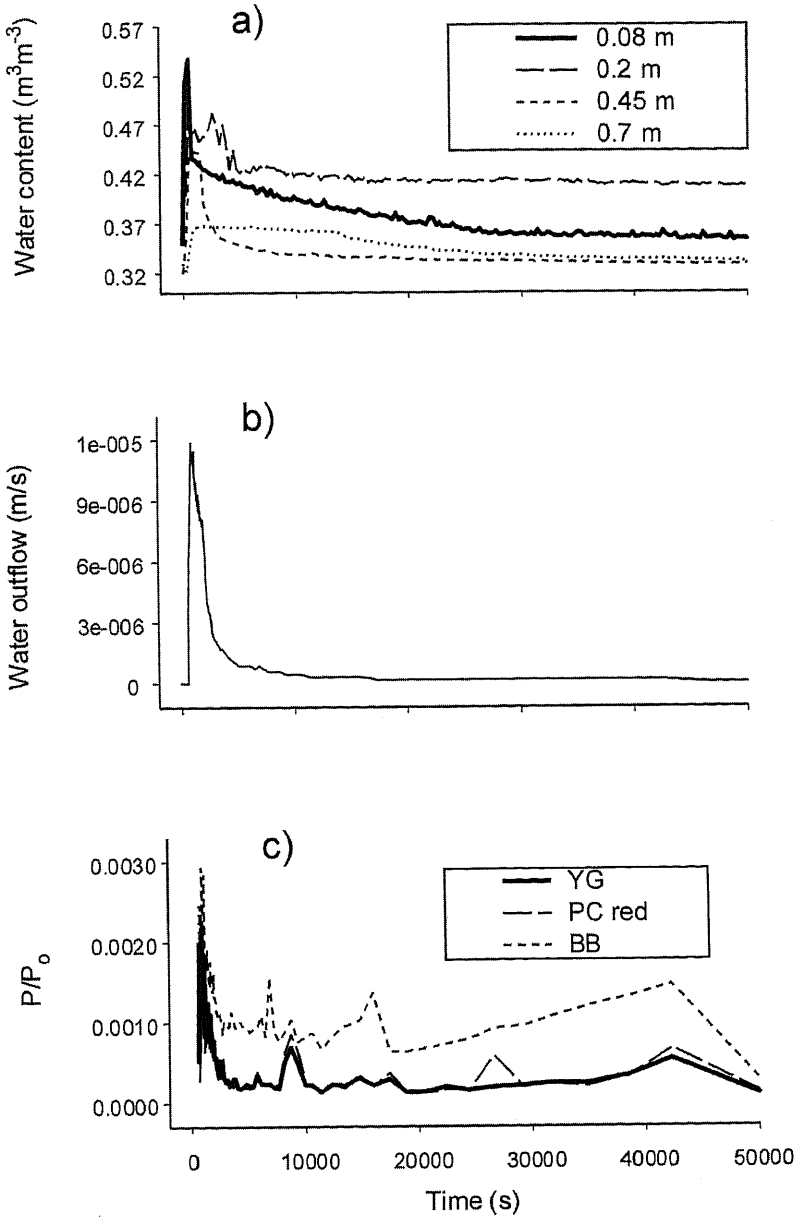

Figure 3. Experiment Bantiger 2, run 1: Observed time dependences of (a) water content at depths 0.08, 0.20, 0.45 and 0.70 m, (b) drainage flow, and (c) relative particle numbers of YG, PC red, and BB recovered in drainage flow. (P_o corresponds to the total of applied particles.)

set to $\Delta t = 300$ s. The phage suspension was applied with a rate $q_S = 7 \times 10^{-6}$ m s^{-1} during $t_S = 7000$ s, leading to a total volume of 3.46 L.

4. Results and Discussion

4.1. Experiment Bantiger 1

[36] Figure 2a shows the depth distributions of the three bead types, demonstrating that they have moved over considerable distances in the soil within approximately one hour after suspension application. YG is more evenly distributed within the profile, whereas the other two types show peaks at the 0.05-to-0.2-m and the 0.35-to-0.7-m depth ranges. However, the three cumulative distributions, Figure 2b, did not significantly differ according to Kolmogorov-Smirnov's test [*Birnbaum*, 1952].

[37] In particular, no significant relationship between the diameters and translocation efficiencies of the three bead types could be established. Mobile soil moisture can be roughly estimated with

$$w = t_W(Z)\frac{q_S}{Z}, \tag{24}$$

where the range of arrival time of the wetting front at depth $Z = 0.7$ m is estimated to $1200 \leq t_W(Z) \leq 3600$ s, leading to $0.08 \leq w \leq 0.24$ m^3 m^{-3}. Most likely q_S is overestimated because water sorption along the flow paths into the finer

Table 5. Parameters Derived From the Application of the Drag Force Approach to Soil Moisture Variations and Drainage Flow

Run, Depth	a	b, m s^{-1}	t_d, s	w m^3 m^{-3}	W, μm	F_d/A, Pa	ℓ/A, km m^{-2}
			Bantiger 2[a]				
From soil moisture at 0.45 m, equation (20)							
1	2.0	5×10^{-4}	1485	0.100	5.0	2.5×10^{-7}	57.0
2	2.0	9×10^{-4}	1159	0.211	4.0	1.5×10^{-6}	42.0
From drainage flow, equation (19)							
1	3.0	3.267	1200	0.015	21.8	4.1×10^{-6}	0.7
2	2.7	0.894	1300	0.014	10.5	2.8×10^{-6}	1.3
			Colombier[a]				
From soil moisture, equation (20)							
0.10 m	2.0	9.0×10^{-4}	7608	0.090	1.7	5.7×10^{-7}	43.0
0.46 m	2.6	2.8×10^{-3}	7275	0.038	4.7	7.4×10^{-7}	24.0
0.58 m	2.2	1.7×10^{-3}	7176	0.029	2.5	1.7×10^{-6}	31.0
From K_S, Table 4 and equations (25), (6), and (3)							
0.30 m	3.00[b]	7.8×10^{-5}	–	–	–	5.4×10^{-8}	140.0
From drainage flow, equation (19)							
0.70 m	2.3	1.584	7210	0.005	4.6	5.2×10^{-6}	1.0

[a] The Kinematic Wave Approach was not applicable to the data at depths 0.08, 0.2, and 0.7 m (Bantiger 2) and at depth 0.3 m (Colombier) due to the discrepancy between model assumptions and observations (see Figures 2 and 6).
[b] Assumed value.

pores of the matrix reduces w and q. The conservative estimate, equation (24), demonstrates that PV between 0.41 and 0.53 m^3 m^{-3} (Table 1) is not a well suited parameter for linking distance with time of colloid traveling in this unsaturated soil.

4.2. Experiment Bantiger 2, Runs 1 and 2

[38] Soil moisture variations at the four depths, drainage outflow, and relative particle number in the effluent of run 1 are shown in Figure 3. The model parameters a and b follow from the application of equations (18) to (23) to moisture variation and drainage flow. They are compiled in Table 5 and indicate typical preferential flow i.e., $2 < a < 3$, according to *Germann and Di Pietro* [1996].

[39] Momentum dissipation dominated flow, and drag forces acted on the particles. The drag force per cross-sectional area of soil, $F_d(t)/A$, follows from the application of equation (6) to either soil moisture variations or drainage flow, using the parameters from Table 5. During particle break through, three phases of $F_d(t)/A$ are discernible from Figure 4a: (1) the increasing limb, (2) the recessing limb, and (3) the trailing phase. Figures 4b to 4d show for each phase the ratios of recovered to applied latex beads, P/P_0, versus $F_d(t)/A$.

4.2.1. Increasing Limb

[40] The particle numbers P/P_0 varied around their averages during the corresponding increase of $F_d(t)/A$, showing slightly decreasing trends. Further interpretation is not appropriate when looking at the short time period of suspension application, $t_S = 900$ s, and the correspondingly short travel time of the wetting front to the bottom of the column, $t_W(Z) = 620$ s, vis-à-vis the time steps of recording soil moisture of $\Delta t = 300$ s.

4.2.2. Recessing Limb

[41] P/P_0 followed linearly the decrease of $F_d(t)/A$ with the coefficients of determination in the range of $0.785 \leq r^2 \leq 0.9$. The slopes of the three linear regressions, as they are indicated in Figures 4b to 4d, do not show significant differences among the three bead types. This is in accord with the results of the experiment Bantiger 1, which also showed no discrimination effects of particle diameters.

4.2.3. Trailing Phase

[42] Beads are still arriving at the bottom of the column despite $q(Z, t)$, and thus $F_d(t)/A$, approaching zero. We assume that the beads were carried by water films, which were torn off from either the pore walls or from slower moving water.

[43] Run 1 of experiment Bantiger 2 demonstrates that drag forces can explain particle transport in soils, mainly during recession. The frequently observed monotonous temporal variations of moisture during recession coincide here with similar smooth behavior of particle loads. Interpreted with caution, we think that flow in macroporous systems is better organized during recession than during infiltration. Once all the water has entered the system, it seems that internal forces acting on the water are smoothing flow at the column scale. In contrast, during infiltration flow may be dominant by additional dynamic forces which are related with pressure and velocity fluctuations at smaller scales.

[44] Compared with run 1, Figure 5 reveals weaker relations between $F_d(t)/A$ and P/P_o during run 2, although the general trend during the recessing limb is still recognizable. The results of run 2 suggest that additional factors need to be considered, and entrainment must be among them. The particles were already suspended in run 1, whereas the flow of run 2 had to pick them up wherever they had previously settled. Thus the spatial distribution of particles prior to, and local flows during, infiltration are thought to be decisive for entrainment and transport efficiency.

[45] Turbulent flow would enhance entrainment, but *Germann* [1990] found Reynolds numbers inferior to 1000 during preferential flow when the thickness of the water films are less than 1 mm. The application of equations (5) and (6) to the soil moisture data results in film thickness in the range of $4 < W < 22$ μm (Table 5), and thus flow was definitely laminar. It is interesting to note that the computed film thicknesses were about twice to 25 times the diameter

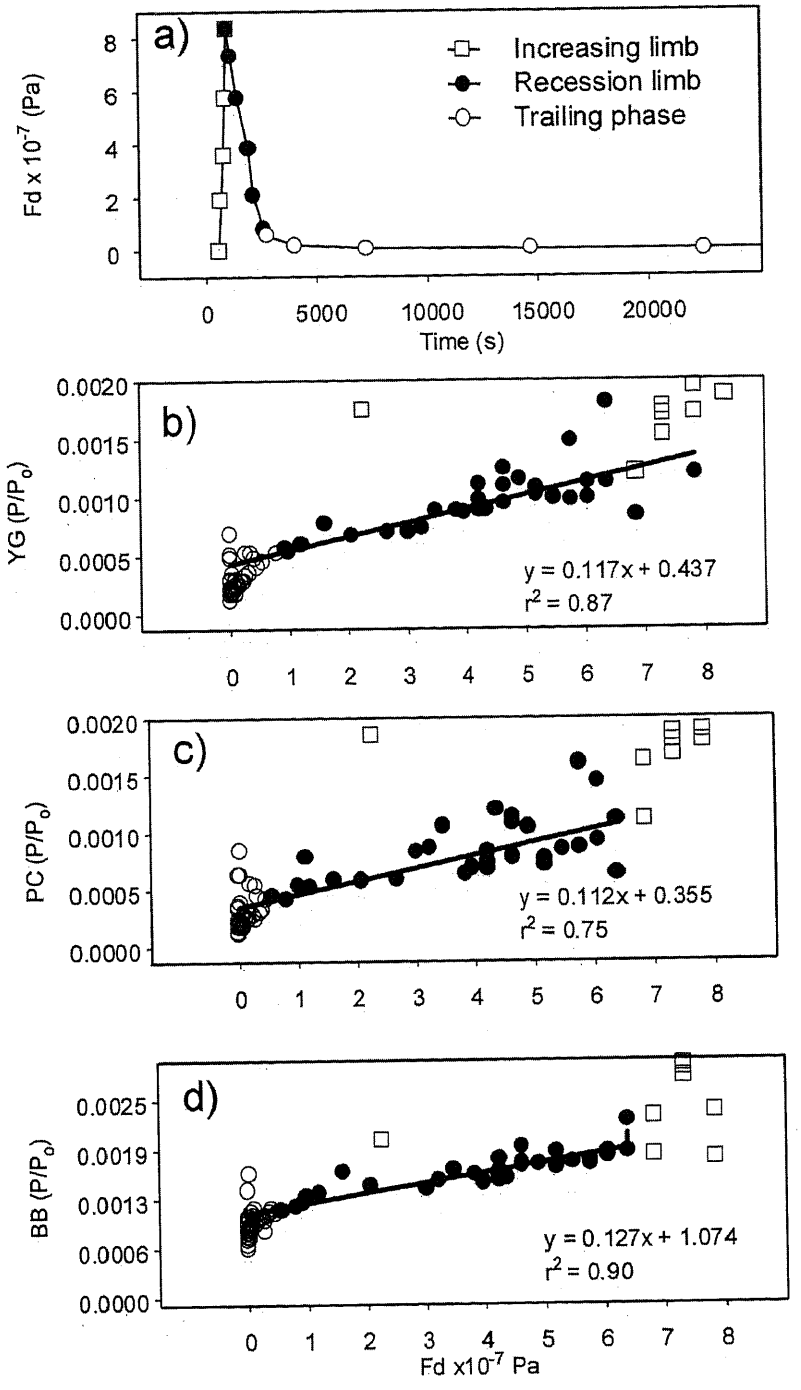

Figure 4. Experiment Bantiger 2, run 1: (a) evolution of F_d/A versus time; (b–d) relative particle numbers of YG, PC red, and BB versus F_d/A.

of the transported beads, thus capable of carrying them efficiently along the flow paths. The ratios of film thickness to particle diameters thus corresponded to the case 1 of *Veerapaneni et al.* [2000].

[46] The F_d/A values calculated from soil moisture variations were 2.5×10^{-7} Pa and 1.5×10^{-7} Pa for runs 1 and 2, respectively (Table 5). They are about two to fifteen times smaller than those estimated from drainage flow with corresponding larger ℓ/A values. The nearly saturated matrix zone at the bottom of the soil column presumably enhances preferential flow, mainly by reducing contact lengths at the same flow rates.

4.3. Experiment Colombier

[47] Figure 6a indicates steady drainage between about 3600 and 7300 s after the onset of sprinkling. Breakthrough shows various behaviors of the bacteriophages (Figures 6b to 6d). The portions of the total of recovered to applied phages were relatively low i.e., 1.13% for H40/1, 1% for H6/1, 0.21% for H4/4, 0.10% for T7 and 0.002% for f1.

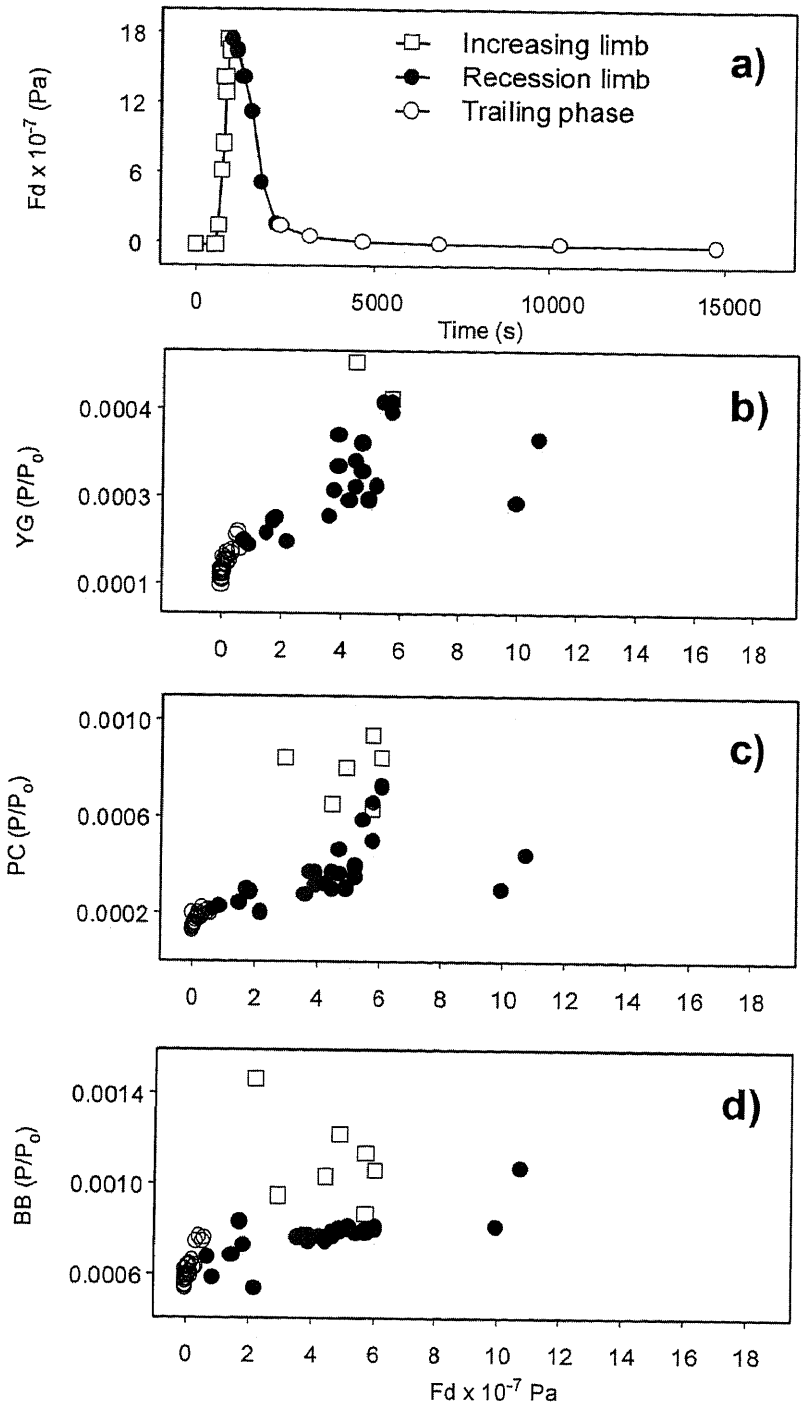

Figure 5. Experiment Bantiger 2, run 2: (a) evolution of F_d/A versus time; (b–d) relative particle numbers of YG, PC red, and BB versus F_d/A.

[48] The evolution of soil moisture is shown in Figure 7, indicating typical preferential flow at the 0.10-m depth with a rapid increase during infiltration to steady state, which is followed by a concave decrease shortly after the cessation of infiltration.

[49] There is hardly any reaction on infiltration at the 0.3-m depth, indicating steady flow in a highly saturated layer without showing the hydraulic reactions of transient preferential flow. Soil moisture reacted more gradually to infiltration at 0.46 and 0.58 m. The layer of sandy clay-loam between 0.28 and 0.36 m does not hamper flow because its saturated hydraulic conductivity is higher than, but close to, the infiltration rate (Table 3). It presumably acted as phage filter.

[50] Figure 8 shows qualitatively the relations between the relative numbers of recovered colloids, P/P_o, with the drag force $F_d(t)/A$. The increasing limb of $F_d(t)/A$ effects positively the amounts of transported particles, Figures 8b to 8f. Compared with runs 1 and 2 of the Bantiger 2 experiment, the relation is better visible because of the wider spread in time of the collected data.

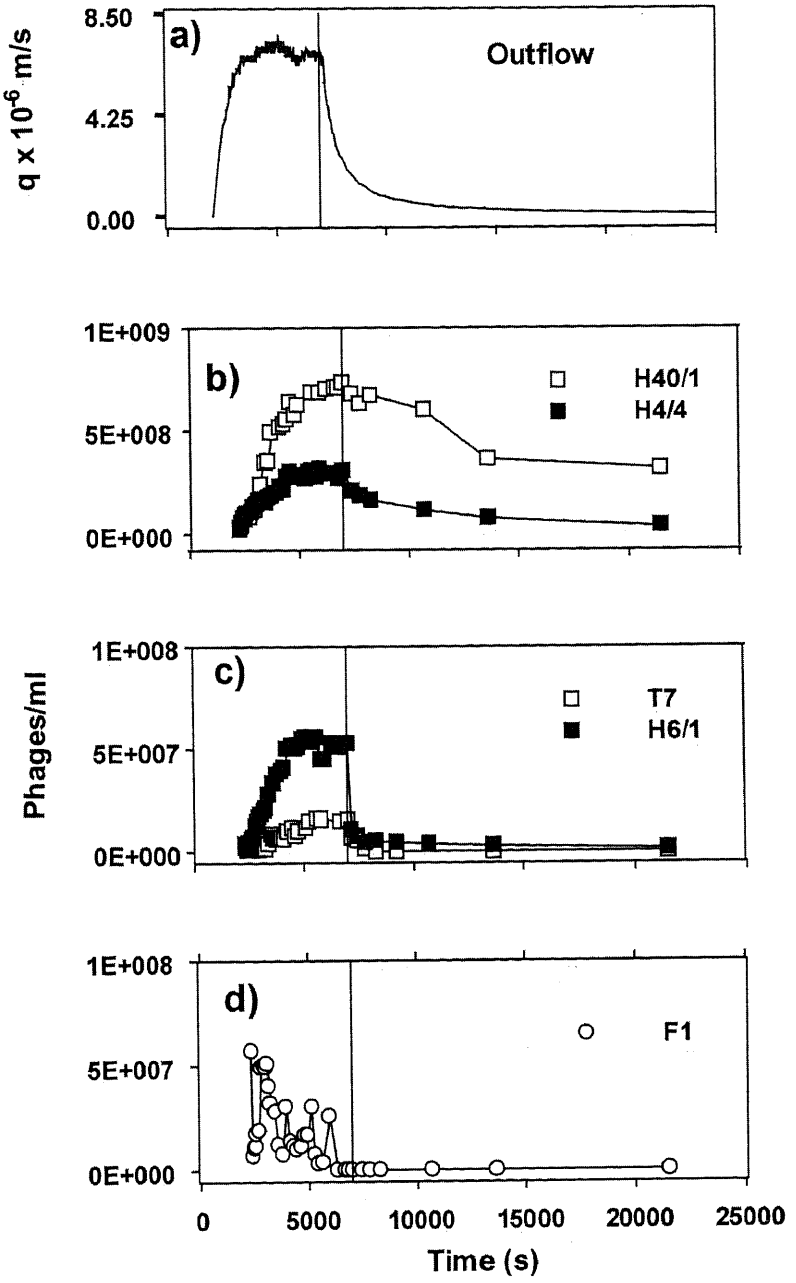

Figure 6. Experiment Colombier: Observed time dependences of (a) drainage flow; (b–d) numbers of five bacteriophages per ml of effluent.

[51] The coherence of P/P_0 versus $F_d(t)/A$ decreases along the sequence of decreasing ratios of recovered colloids from the types H4/4, H6/1, H40/1, T7, and to f1. Figure 8f demonstrates best that the lowest total relative colloid recovery of the phage f1 of only 0.002% is the most weakly related with the drag force. The increase of colloid sorption thus seems related to the decrease of the impact of the drag forces on colloid transport. However, there is currently not enough information to further explore relations between the ξ potential, hydrophobicity, and other properties of the phages and their hosts to better explain their transportation behaviors. The proton charges on the solid surfaces and the pH of the mobile water are thought additional important parameters controlling colloid retention.

[52] The following considerations may highlight the effect of the layer between 0.28 and 0.36 m on flow and transport. The contact length of mobile water per cross sectional area of soil, ℓ/A, is a measure for momentum transfer from mobile water towards the parts at rest: The longer the line the more pronounced momentum will dissipate and hence the reduction of conductivity. The parameter ℓ/A follows from equation (3) which was applied to the soil moisture variations at depths 0.1, 0.46, and 0.58 m. In the case of the highly saturated layer at the 0.3-m depth, ℓ/A is estimated from the layer's intrinsic permeability

$$k = K_S \frac{\eta}{g} \tag{25}$$

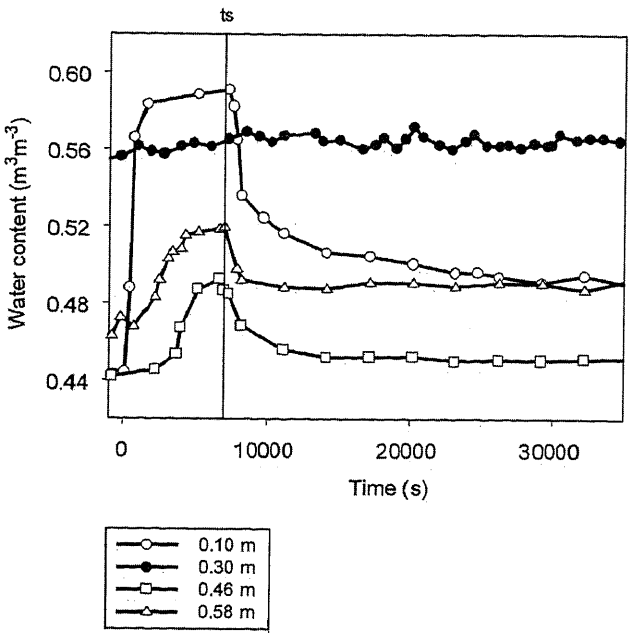

Figure 7. Experiment Colombier: Observed time dependence of soil moisture at depths 0.1, 0.3, 0.46, and 0.58 m. Approximate constant soil moisture at depth 0.3 m indicates flow in the sand layer close to water saturation.

m^2 [see, e.g., *Freeze and Cherry*, 1979]. The comparison of equations (25) and (3) leads to

$$\frac{\ell}{A} = \sqrt{\frac{1}{2ak}}. \tag{26}$$

Under the assumption that $a = 3$, the corresponding contact length ℓ/A and drag force F_d/A per cross sectional area amount to 1.4×10^5 m^{-1} and 5.4×10^{-8} Pa, respectively. The latter is at least 10 times smaller than the drag forces above and below the filtering layer and the former accordingly longer, as compiled in Table 5. The greater ℓ/A the more pronounced are momentum dissipation, F_d/A reduction, and the probability of colloid retention. Tortuosity is most likely also related with ℓ/A, however, currently not further specifiable.

4.4 Comparison With a Previous Study

[53] *Germann et al.* [1987] applied a kinematic wave approach to the transport of *Escherichia coli*, strain K12, with colloid diameters of about 2 μm. Colloid breakthrough was investigated from a total of 19 columns of undisturbed soils with lengths varying from to 0.23 to 0.31 m. The columns were collected at four different sites, representing three different soil types. Drag forces were not considered at that time, and only drainage flow and colloid recovery from

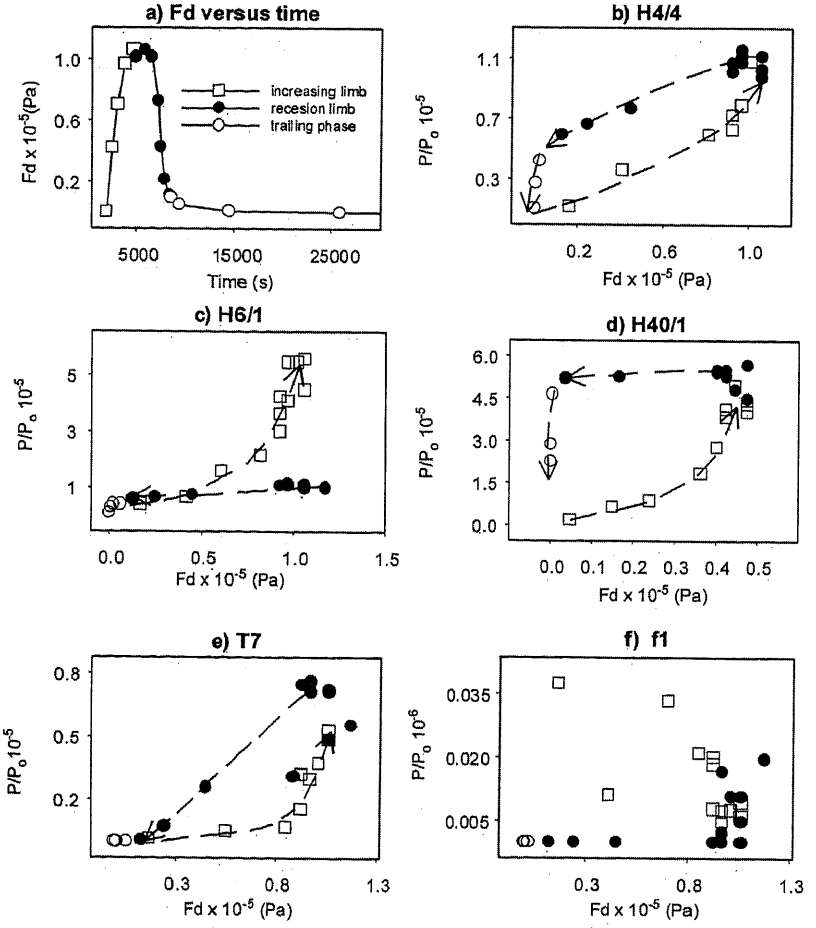

Figure 8. Experiment Colombier: (a) evolution of F_d/A versus time; (b–f) relative numbers of bacteriophages versus F_d/A.

Table 6. Parameters of *Escherichia coli* Breakthrough[a]

Run Number	b,[b] $\times 10^{-3}$ m s^{-1}	w,[b] m^3 m^{-3}	$q(Z)$,[b] $\times 10^{-6}$ m s^{-1}	W,[c] μm	F_d/A,[d] $\times 10^{-7}$ Pa	ℓ/A,[e] km m^{-2}	C/C_o[b]
			Typic Paleudalf				
1	9.2	0.050	5.22	3.4	2.6	14.6	0.23
2	1568.0	0.006	5.35	5.4	15.9	1.1	0.14
3	26.7	0.033	5.19	3.8	4.2	8.6	0.23
4	508.0	0.010	5.26	5.1	12.9	2.0	0.20
5	2.9	0.104	10.00	4.0	4.9	26.0	0.32
6	86.0	0.017	3.05	3.6	3.1	4.8	0.11
7	391.0	0.007	1.40	3.1	1.8	2.2	0.05
8	342.0	0.012	5.38	5.0	12.1	2.4	0.23
9	574.0	0.010	5.40	5.4	16.5	1.8	0.22
10	2.6	0.086	5.54	3.1	1.8	27.5	0.34
			Cumulic Hapluquoll				
11	24.5	0.044	10.00	4.9	11.2	8.9	0.23
12	106.0	0.018	4.75	4.2	5.9	4.3	0.81
			Typic Udifluvent				
13	214.0	0.019	10.40	6.3	29.8	3.0	0.81
14	120.0	0.018	5.22	4.5	7.6	4.0	0.79
			Typic Paleudalf				
15	0.5	0.018	5.22	2.9	0.0	62.6	0.49
16	256.0	0.018	10.10	6.5	34.4	2.8	0.68
17	4.7	0.065	5.11	3.2	2.0	20.4	0.20
18	140.0	0.018	5.70	4.8	10.3	3.7	0.65
19	60.2	0.013	1.12	2.3	0.5	5.7	0.07

[a] See *Germann et al.* [1987].
[b] According to *Germann et al.* [1987]; the exponent $a = 2.5$ was kept constant, and C/C_o refers to the bacteria concentration during steady drainage, relative to the input concentration.
[c] Equation (4).
[d] Equation (6).
[e] Equation (3).

the column bottoms were recorded. The pertinent results of the experiments, and the parameters of the drag force approach derived thereof, are summarized in Table 6. The flow and drag force parameters are in the same ranges as those in Table 5.

[54] However, Figure 9 shows a broad variation in the relation of P/P_0 versus $F_d(t)/A$. The arbitrary separation into the two groups of $F_d(t)/A < 10^{-6}$ Pa and $F_d(t)/A > 10^{-6}$ Pa may hint at some threshold values of the parameters involved in the efficiency of bacterial transport. On the other side, soil sites and types are found in both groups, indicating that site and soil type are not necessarily related with transport efficiency.

5. Conclusions

[55] We developed a fluid mechanical approach to the transport of colloids in unsaturated soils which resulted in a particle-pushing drag force. We presented the data of three types of experiments. In experiment Bantiger 1 we sprinkled in situ a suspension of three types of latex beads and methylene blue on the surface of a forest soil. Sampling immediately after suspension application revealed that the colloids had moved approximately within an hour to a depth of at least 0.7 m. The estimated range of mobile soil moisture related with the colloid transport amounted to $0.08 \leq w \leq 0.24$ m^3 m^{-3}, which is utmost half the porosity i.e., the fast and far-reaching colloid translocations involved only a part of the porosity. This fact supports the drag force approach to transient flow in unsaturated soils, which assumes rapid flow to occur in films and rivulets along preferred flow paths with a minor fraction of soil moisture involved in the flow process. Thus, in accord with *Wan and Wilson* [1992], *Wan and Tokunaga* [1997], and *Veerapaneni et al.* [2000] total pore volume, PV, seems not to be an appropriate parameter for modeling the transport of colloids through unsaturated porous media.

[56] The three bead diameters did not discriminate colloid transport during the recession limb of drainage, as experi-

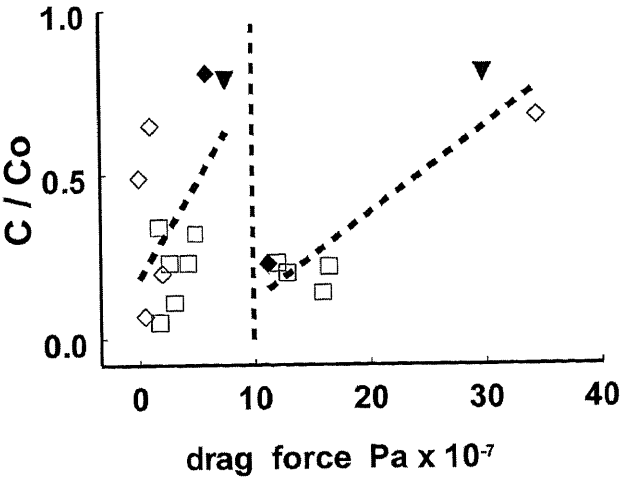

Figure 9. Relative concentration of *Escherichia coli* versus drag force [from *Germann et al.*, 1987]. The arbitrary separation at 10^{-6} Pa may illustrate the soil specific effects on colloid transport.

ment Bantiger 2, run 1 (Figure 4) showed. The three bead types shared the same physicochemical properties, mainly by not having surface charges. Thus similar relations of P/P_o versus $F_d(t)/A$ resulted, as we think, mainly because the films of flow were distinctly thicker than the diameters of the colloids. The results correspond with the case of completely submerged spheres with the diameters smaller than film thickness as described by *Veerapaneni et al.* [2000]. The interpretation indicates a more general applicability of the drag force approach to the transport of colloids if they are applied in suspension. The experiment Bantiger 2, run 2 (Figure 5) demonstrates that there are still no differences discernible among the three bead types. However, the relations P/P_o versus $F_d(t)/A$ got fuzzier when the infiltrating bead-free water had to entrain colloids which had previously settled within the soil. The places of entrainment during the second run were spread along the soil column. The distances the colloids had to travel were thus distributed between the entire length of the soil column and any fractions of it. The varying distances do not allow to properly compute the relation between arrival times and the drag forces acting on the colloids. (One could run the model in the reverse mode to arrive at the depth distributions of the colloid pick-up sites, however, this intriguing perspective seems too speculative vis-à-vis the current limited experience with the drag force approach.)

[57] Finally, the bead diameters did not discriminate the depth distributions in experiment Bantiger 1, thus supporting the noneffect of particle diameters found with experiments Bantiger 2. These results do not confirm the relation between the ratio of particle velocity to maximum fluid velocity on one side and the ratio of particle diameter to film thickness on the other side as *Veerapaneni et al.* [2000]. have found. The heterogeneities of the soil and flow properties most likely overwhelmed the effects of particle size.

[58] In contrast, the Colombier experiment demonstrates the effects of various surface properties on colloid transport, though in a bulky way. The colloid properties acting against the drag forces are simply inferred from the numbers of phages having broken through relative to their numbers applied i.e., the fuzziness of P/P_o versus $F_d(t)/A$ increases with the number of colloids retained during transport, that is $(1 - P/P_o)$.

[59] The hysteretical behavior of P/P_o versus $F_d(t)/A$ during transport of the phages H4/4, H40/1, and T7 is intriguing. At this early stage of experiences with the drag force approach we think that the observed hysteresis is either related to flow path variations when switching from the increasing to the decreasing limbs of transient flow or to some dynamic local colloid retention and entrainment during flow. Further, we demonstrated that the computed film thicknesses were twice to twenty times the colloid diameters. Thus colloid transport may well depend on the distance between the colloids and the resting parts of the system because the velocity of water lamina increases with the square of the distance to the solid-liquid interface. Finally, the comparison with earlier investigations by *Germann et al.* [1987] demonstrated that the model parameters are within the same respective ranges of all experiments presented here. This adds confidence to the drag force approach. However, the wide spread of P/P_o versus $F_d(t)/A$ relations as shown in Figure 9 also indicate the impacts on colloid transport of soil properties not addressed in this study. From this we conclude that the investigation of the spatial variability of the soil properties leading to drag forces might be worthwhile.

[60] From a fluid-mechanical perspective, it was possible to incorporate saturated hydraulic conductivity via intrinsic permeability into the drag force approach. Moreover, the microscopic drag forces directly acting on the colloids are possibly better related with their geometry than the convenient macroscopic definition developed here, as the following numerical exercise may indicate. The diameters of particles range from 0.2 to 2 μm and the drag forces per cross sectional area of soil from 5×10^{-8} to 5×10^{-6} Pa, according to Tables 5 and 6. However, the corresponding forces acting on sessile particles per unit of their cross-sectional area amount to $\approx 10^5 < F_P < \approx 10^8$ Pa, i.e., to about 1 to 10^3 bar.

[61] The potential of the drag force approach to colloid transport in unsaturated soils lies in its relating dynamic fluid properties with transport efficiency. However, there is a long way to go to achieve the elegance of coupling transport with retention of colloids in soils as they were presented, for instance, by *Hornberger et al.* [1992], *Corapcioglu and Choi* [1996], and *Grolimund and Berkovec* [2001].

[62] **Acknowledgments.** The Swiss National Science Foundation generously supported our efforts with the grants numbers 21-36281.92 and 21-29725.90. We deeply appreciate Pierre Rossi's contribution from the Laboratory of Microbiology at the University of Neuchâtel who prepared the virus stocks, purified and counted the phages. The efforts of two anonymous reviewers helped to more clearly present our case.

References

Birnbaum, Z. W., Critical values for the Kolmogorov-Smirnov test statistics, *J. Am. Stat. Assoc.*, *47*, 425–441, 1952.

Corapcioglu, M. Y., and H. Choi, Modeling colloid transport in unsaturated porous media and validation with laboratory column data, *Water Resour. Res.*, *32*, 3437–3449, 1996.

Di Pietro, L., and F. LaFolie, Water flow characterization and test of a kinematic wave model for macropore flow in a highly contrasted and irregular double-porosity medium, *J. Soil Sci.*, *42*, 551–563, 1991.

Freeze, R. A., and J. A. Cherry, *Groundwater*, Prentice-Hall, Old Tappan, N. J., 1979.

Gerba, C. P., and G. Bitton, Microbial pollutants: Their survival and transport pattern to groundwater, in *Groundwater Pollution Microbiology*, edited by G. Bitton and C. P. Gerba, John Wiley, New York, 1984.

Germann, P. F., Kinematic wave approach to infiltration and drainage into and from soil macropores, *Trans. Am. Soc. Agric. Eng.*, *28*(3), 745–749, 1985.

Germann, P. F., Preferential flow and the generation of runoff, 1, Boundary-layer flow theory, *Water Resour. Res.*, *26*, 3055–3063, 1990.

Germann, P. F., A hydromechanical approach to preferential flow, in *Model Validation: Perspectives in Hydrological Sciences*, edited by M. G. Anderson and P. D. Bates, pp. 233–260, John Wiley, New York, 2001.

Germann, P. F., and L. Di Pietro, When is porous media preferential? A hydromechanical perspective, *Geoderma*, *74*, 1–21, 1996.

Germann, P. F., and L. Di Pietro, Scales and dimensions of momentum dissipation during preferential flow in soils, *Water Resour. Res.*, *35*, 1443–1454, 1999.

Germann, P. F., and L. L. Douglas, Comment on "Particle Transport Through Porous Media" by Laura M. McDowell-Boyer, James R. Hunt, and Nicholas Sitar, *Water Resour. Res.*, *23*, 1697–1698, 1987.

Germann, P. F., M. S. Smith, and G. W. Thomas, Kinematic Wave approximation to the transport of *Escherichia coli* in the vadose zone, *Water Resour. Res.*, *23*, 1281–1287, 1987.

Germann, P. F., E. Jäggi, and T. Niggli, Rate, kinetic energy and momentum of preferential flow estimated from in-situ water content measurements, *Eur. J. Soil Sci.*, in press, 2002.

Ginn, T. R., Comment on "Stochastic analysis of virus transport in aquifers" by Linda L. Campbell Rehmann, Claire Welty, and Ronald W. Harvey, *Water Resour. Res.*, *36*, 1981–1982, 2000.

Grolimund, D., and M. Berkovec, Release and transport of colloidal particles in natural porous media, 1, Modeling, *Water Resour. Res.*, *37*(3), 559–570, 2001.

Grolimund, D., K. Barmettler, and M. Berkovec, Release and transport of colloidal particles in natural porous media, 2, Experimental results and effects of ligands, *Water Resour. Res.*, *37*, 571–582, 2001.

Gvirtzman, H., and S. M. Gorelick, Dispersion and advection in unsaturated porous media enhanced by anion exclusion, *Nature*, *352*, 793–795, 1991.

Hornberger, G. M., A. L. Mills, and J. S. Herman, Bacterial transport in porous media: Evaluation of a model using laboratory observations, *Water Resour. Res.*, *28*, 915–938, 1992.

Jacobsen, O. H., P. Moldrup, C. Larsen, L. Konnerup, and L. W. Petersen, Particle transport in macropores of undisturbed soil columns, *J. Hydrol.*, *196*, 185–203, 1997.

Lighthill, G. J., and G. B. Whitham, On kinematic waves, I, Flood movement in long rivers, *Proc. Br. R. Soc., Ser. A*, *229*, 281–316, 1955.

McDowell-Boyer, L. M., J. R. Hunt, and N. Sitar, Particle transport through porous media, *Water Resour. Res.*, *22*, 1901–1921, 1986.

Mdaghri-Alaoui, A., Transferts d'eau et de substances (bromures, chlorures et bactériophages) dans des milieux non saturés à porosité bimodale: Expérimentation et modélisation, Ph.D. dissertation, 148 pp., Fac. of Sci., Univ. of Bern, Bern, 1998.

Rahe, T. M., C. Hagedorn, E. L. McCoy, and C. F. Kling, Transport of antibiotic resistant *Escherichia coli* through a western Oregon hill slope under conditions of saturated flow, *J. Environ. Qual.*, *7*, 687–694, 1978.

Rehmann, L. L. C., C. Welty, and R. W. Harvey, Stochastic analysis of virus transport in aquifers, *Water Resour. Res.*, *35*, 1987–2006, 1999.

Richards, L. A., Capillary conduction of liquids in porous mediums, *Physics*, *1*, 318–333, 1931.

Riesen, D., Partikeltransport in Böden, Ph.D. dissertation, 136 pp., Fac. of Sci., Univ. of Bern, Bern, 1995.

Rossi, P., Advances in biological tracer techniques for hydrology and hydrogeology using bacteriophages: Optimization of the methods and investigation of the behaviour of the bacterial viruses in surface waters and in porous and fractured aquifers, Ph.D. dissertation, 200 pp., Fac. of Sci., Univ. of Neuchâtel, Neuchâtel, Switzerland, 1994.

Roth, K., R. Schulin, and W. Attinger, Calibration of time domain reflectrometry for water content measurement using a composite dielectric approach, *Water Resour. Res.*, *26*, 2267–2274, 1990.

Saiers, J. E., G. M. Hornberger, and L. Liang, First- and second-order kinetic approaches for modeling the transport of colloidal particles in porous media, *Water Resour. Res.*, *30*, 2499–2506, 1994.

Schäfer, A., P. Ustohal, H. Harms, F. Stauffer, T. Dracos, and A. J. B. Zehnder, Transport of bacteria in unsaturated porous media, *J. Contam. Hydrol.*, *33*, 149–169, 1998.

Seta, A. K., and A. D. Karathanasis, Stability and transportability of water-dispersible soil colloids, *Soil Sci. Soc. Am. J.*, *61*, 604–611, 1997.

Smith, M. S., G. W. Thomas, R. E. White, and D. Ritonga, Transport of *Escherichia coli* through intact and disturbed columns of soil, *J. Environ. Qual.*, *14*, 87–91, 1985.

Shrauf, T. W., and D. D. Evans, Laboratory studies of gas flow through a single natural fracture, *Water Resour. Res.*, *22*, 1038–1050, 1986.

Toran, L., and A. V. Palumbo, Colloid transport through fractured and unfractured laboratory sand columns, *J. Contam. Hydrol.*, *9*, 289–303, 1992.

Veerapaneni, S., J. Wan, and T. K. Tokunaga, Motion of particles in film flow, *Environ. Sci. Technol.*, *34*(12), 2464–2471, 2000.

Wan, J., and T. K. Tokunaga, Film straining of colloids in unsaturated porous media: Conceptual model and experimental testing, *Environ. Sci. Technol.*, *31*(8), 2413–2420, 1997.

Wan, J., and J. L. Wilson, New findings on particle transport within the vadose zone: The role of the gas-water interface, in *Proceedings of the Twelfth Annual American Geophysical Union Hydrology Days, March 31 to April 3, Fort Collins, Colorado (USA)*, edited by H. J. Morel-Seytoux, pp. 402–419, Hydrology Days, Atherton, Calif., 1992.

White, R. E., The transport of chloride and nondiffusible solutes through soil, *Irrig. Sci.*, *6*, 3–10, 1985.

A. Alaoui and P. F. Germann, Soil Science Section, Department of Geography, University of Bern, Hallerstrasse 12, CH-3012 Bern, Switzerland. (germann@giub.unibe.ch)

D. Riesen, BCD GmbH, Belpstrasse 34, 3007 Bern, Switzerland.